Polyether–Polyimide Thermoplastic Elastomers. I. Synthesis and Properties

XUEHAI YU,[1] CHUNKANG SONG,[1] CHI LI,[2,*] and STUART L. COOPER[2,†]

[1]Chemistry Department, Nanjing University, People's Republic of China and [2]Chemical Engineering Department, University of Wisconsin, Madison, Wisconsin 53706

SYNOPSIS

A series of polyether–polyimides based on polycondensation of poly(tetramethylene oxide)glycol di-*p*-aminobenzoate with different molecular weights (650, 1000, 2000) and benzenetetracarboxylic acid dianhydride (BTDA) or 3,3',4,4'-benzenetetracarboxylic acid anhydride (BPTDA) was synthesized. Infrared spectroscopy (IR), differential scanning calorimetry (DSC), dynamic mechanical analysis (DMA), and stress–strain tests were used to follow the imidization process and to study the structure–property relations of this family of polymers. FTIR data showed that the imidization was completed after 6 h at 140°C, which is a much lower temperature than that required for polyimides synthesized from low molecular weight diamines. DSC and DMA results indicated that the block copolymer exhibited a well-phase-separated structure and had a broad rubbery plateau from about −70°C to 260°C, which varied with dianhydride type and hard-segment content. The BTDA series had enhanced mechanical properties compared to the BPTDA series. The excellent tensile properties of the polyether–polyimides suggest that they could be potentially used as heat-resistant thermoplastic elastomers.

INTRODUCTION

Elastomeric thermoplastic block copolymers are typically microphase-separated materials containing two types of segments in their molecular architecture. The hard and soft segments alternately appear in the polymer backbones, which can be described as an $(A-B)_n$ multiblock polymer. The hard segments, represented as A, form a glassy or semicrystalline microphase and serve as reversible physical crosslinks. The soft segments, B, are in a rubbery state at service temperature and impart flexibility to these copolymers.[1] A typical thermoplastic block copolymer can contain polyether, polyester, polyalkyl, or polysiloxane as the soft segment, while the hard segments can possess urethane, amide, urea, or carbonate moieties.[2] The lower limit of service temperatures of these block copolymers is determined by the glass transition temperature, T_g, of the soft segment, while the hard-segment T_g or melting temperature governs the upper limit of service temperature. Recent efforts have been aimed to extend the service temperature range of block copolymers by broadening their rubbery plateau by either using low T_g soft segments and/or high T_g hard segments.

Aromatic polyimides generally exhibit melting or decomposition temperatures higher than 350°C. They also possess excellent solvent resistance, mechanical strength, and electrical properties. Recent research efforts have focused on improving the processibility of the polyimides by introducing structural variations into their backbone.[3–5] Only a few papers describe the incorporation of polyimide segments into thermoplastic block copolymers. Masiulanis et al. synthesized polyurethane–imides by reacting isocyanate-tipped polyurethane oligomers with dianhydride of pyromellitic acid (BTDA).[6] Yilgor and McGrath prepared segmented polysiloxane–polyimide block copolymers by condensing amine-

* Present address: Scientific Research Laboratories, Ford Motor Company, Dearborn, MI 48121.
† To whom correspondence should be addressed.

Journal of Applied Polymer Science, Vol. 44, 409–417 (1992)
 CCC 0021-8995/92/030409-09$04.00

terminated poly(dimethylsiloxane) with benzophenone–tetracarboxylic acid dianhydride (BPTDA).[7]

A series of poly(ether)–imide block copolymers based on poly(tetramethylene oxide)glycol di-*p*-aminobenzoate soft segments and aromatic polyimide hard segments was synthesized and characterized in this investigation. The soft segments were selected for their reported superior thermal stability as compared to poly(propylene glycols).[8] Polymer synthesis and structure–property relationships were studied by using infrared (IR) spectroscopy, differential scanning calorimetry (DSC), dynamic mechanical analysis (DMA), and tensile testing.

EXPERIMENTAL

Materials

Three different molecular weight samples of poly(tetramethylene oxide)glycol di-*p*-aminobenzoates were kindly provided by G. E. Nicholson of the Polaroid Corporation under the trade name "POLAMINE." The average molecular weights of the samples designated as POLAMINE 650, 1000, and 2000 were 942, 1256, and 1900, respectively. These oligomers were vacuum-dried at 70°C for 24 h and kept in a desiccator before use. BTDA (97% anhydride with the remainder free acid) and BPTDA (98% anhydride) were purchased from Aldrich Chemical Company. The anhydrides were vacuum-dehydrated at 160°C for 6 h before use. Tetrahydrofuran (THF) (Aldrich HPLC grade) was kept dry over molecular sieves (Fisher 4A).

Synthesis

Polyamic Acid

The polycondensation reaction was carried out under a dry argon atmosphere. A solution of 15 wt % dianhydride in THF was added to another THF solution containing a stoichiometric amount of poly(ether diamine). The exothermic reaction raised the temperature to about 40°C after mixing. The solution was stirred at room temperature overnight until FTIR spectra showed that the amine absorption peaks had completely disappeared. A yellowish viscous solution was obtained. The polymer was precipitated in methanol, filtered, and dried. The yield was above 95%.

Poly(ether imides)

The polyamic acid obtained from above synthesis was redissolved in THF and cast onto a Teflon disc. Films of different thickness were dried in air at room temperature. The poly(ether amic acid) was converted to poly(ether imide) in a vacuum oven. The extent of the imidization was followed by FTIR using the —NH— (3320 cm^{-1}) and —COOH (1600 cm^{-1}) peaks. When these peaks completely disappeared, the reaction was completed. The polyimide films can be redissolved in dichloromethane.

Sodium Salt of Polyamic Acid

The polyamic acid was dissolved in dichloromethane and an equimolar amount of sodium acetate dissolved in methanol was added to the solution. The reaction mixture was cast onto a Teflon disc and dried in a vacuum oven at 70°C.

All materials studied are described in Table I. A sample made from "POLAMINE" 650 and BTDA is designated as PI-650–BTDA, and the sodium salt of the same polyamic acid is designated as PA-650–BTDA–Na.

Test Methods

Infrared survey spectra were recorded with a Nicolet 7199 Fourier transform infrared spectrophotometer operated with a dry air purge. Thirty scans at a res-

Table I Materials Studied

Code	MW of Diamine	Dianhydride	Hard Segment (wt %)
PI-650–BTDA	942	BTDA	39
PI-650–BPTDA	942	BPTDA	48
PI-1000–BTDA	1256	BTDA	31
PI-1000–BPTDA	1256	BPTDA	35
PA-1000–BTDA–Na	1256	BTDA	34
PI-2000–BTDA	1900	BTDA	21
PI-2000–BPTDA	1900	BPTDA	25

olution of 2 cm^{-1} were signal-averaged before Fourier transformation.

For kinetic studies, the polyether–polyamic acid based on poly(tetramethylene oxide)glycol diaminobenzoate (M_n = 1256) was mixed with BTDA in a THF solution and cast on salt plates. The solvent was removed in vacuum at ambient temperature. The samples were then placed in vacuum ovens at different temperatures. They were removed from the vacuum oven at various time intervals during the course of the imidization for IR analysis. Absorbance spectra for each sample were obtained using a 5DX FTIR.

Thermal analysis was carried out using a Perkin-Elmer DSC-2C interfaced with a TADS data station. Temperature and enthalpy calibrations were carried out using indium and mercury as standards. A heating rate of 20 K/min under a He purge was used. The data station software allowed automatic subtraction of the base line and normalization of the thermogram for sample weight.

Dynamic mechanical spectra were obtained using a Rheovibron DDV-II apparatus that was controlled by a computer. All measurements were carried out under a nitrogen purge at a frequency of 110 Hz with a constant heating rate of 2°C/min.

Room temperature uniaxial stress–strain data were taken on an Instron table model tensile device using a crosshead speed of 0.5 in./min. Dumbbell-shaped samples with a gauge length of 0.876 in. were stamped out with an ASTM D-1708 die.

RESULTS AND DISCUSSION

Synthesis

The reaction schemes and polymer structures are illustrated in Figure 1. The progress of the imidization reaction was monitored by using FTIR spectroscopy. The FTIR bands at 3320 cm^{-1} (N—H absorbance), 1540 cm^{-1} (amide II band), and 1600 cm^{-1} (—COOH absorbance) were used to evaluate the disappearance of amic acid as shown in Figure 2. As the amic acid is converted to imide, the intensity of these peaks decreases while a characteristic imide peak appears at 1770 cm^{-1}.[7] The IR experiment suggests that imidization was completed at 140°C after 6 h. No change occurred in the IR spectra with further increases in temperature or reaction time. The imidization reaction of this polymer proceeds much faster as compared to conventional polyimides.[9] The results suggest that introducing polyether soft segments into the polyamic acid backbone increases its mobility, which makes the amic acid groups more reactive. The kinetics of the imidization will be discussed later.

Dynamic Mechanical Analysis

Figure 3 shows typical dynamic mechanical spectra of PI–BTDA-1000 that has undergone the imidization process for different temperatures and times. Before curing, the polyamic acid is a one-phase material with a loss tangent peak around 30°C. After heating at 70°C for 36 h, a distinct rubbery plateau appears, indicating that phase separation has occurred. The β-peak of the soft-segment-phase glass transition shifts to lower temperature and a new α-peak at higher temperature appears. An increase in the storage modulus (E') at about 200°C can be observed, suggesting that imidization was continuing to proceed during thermal scanning. After the material was heated to 140°C for 2 h, the β-peak shifted to lower temperatures, whereas in the plateau region, the values of the elastic modulus increased together with broadening of the plateau modulus temperature range. This indicates that the phase-separation progresses further as a result of an increase in the extent of imidization. After heating the material for 6 h at 140°C, the position of the β-peak remains at the same temperature while its intensity decreases. Further increases in the rubbery plateau modulus and hard-segment T_g can be observed as the imidification and the phase separation reach completion. No change in dynamic mechanical properties was observed when the poly(ether)–imide material was heated in vacuum at 140°C for a longer period of time, indicating that both the imidization reaction and the microphase separation reached completion at 140°C after 6 h. This result is consistent with the FTIR data. There also appears to be a high-temperature rubbery plateau above the α-transition, which implies that the sample is partially cross-linked.

Figure 4 shows a comparison of the viscoelastic properties of two samples with different hard segments, BTDA-1000 and BPTDA-1000, having the same cure conditions. Block copolymers with BPTDA hard segments possess a higher hard-segment volume fraction than do the BTDA-based polymers. The BTDA sample, however, exhibits a higher plateau modulus, a higher level of phase separation, and a wider plateau temperature range than does BPTDA-based material. This suggests that molecular rigidity of the hard segment can play a significant role in determining the physical properties of this system.

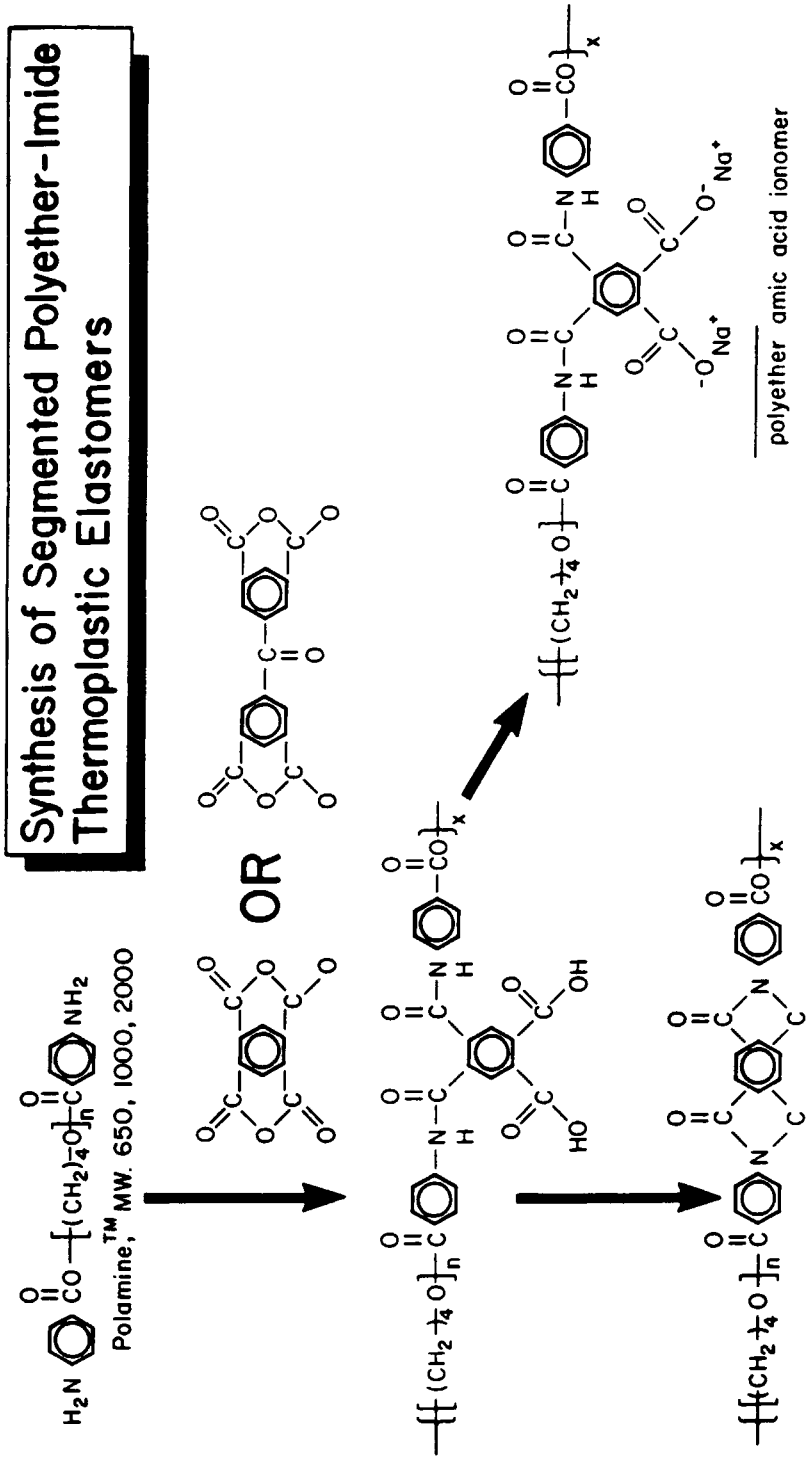

Figure 1 Synthesis and properties of segmented polyether-polyimide thermoplastic elastomers.

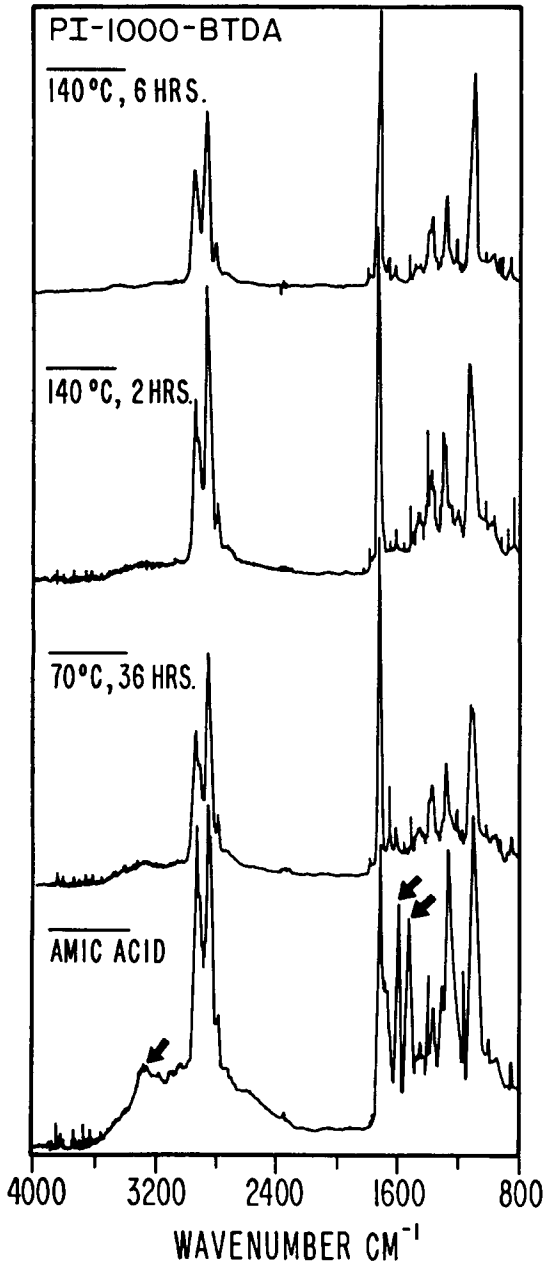

Figure 2 FTIR spectra of PI-1000–BTDA after curing at various conditions.

Figure 5 displays the temperature dependence of the storage modulus, E', and the loss factor, tan δ, of three BPTDA-based materials with different soft-segment molecular weights. The curves show a mechanical relaxation region due to micro-Brownian motions of the PTMO soft segments in each copolymer. The loss peak is shifted to lower temperature and becomes narrower in width with increasing polyether molecular weight. This indicates that the phase separation between the soft and hard segments becomes more complete with an increase in PTMO molecular weight. Since the rubbery plateau modulus is determined by the continuous portion of the hard-segment phase, an increase in soft-segment volume fraction will cause a decrease of the plateau modulus as expected.

Thermal Analysis

DSC curves for both the BTDA and the BPTDA series of polymers are shown in Figure 6, and the thermal transition data are summarized in Table II. All DSC data are for the first heating of the samples. The breadth of the soft-segment T_g provides a qualitative measurement of soft-phase homogeneity. A decrease in soft-segment T_g and a decrease in its breadth are observed as the molecular weight of the soft segment increases. The low-temperature T_g for the BTDA-based polymers is much lower than those of the BPTDA-based polymers, suggesting that the BTDA-based materials have better phase separation than do the BPTDA-based samples at the same polyether soft-segment molecular weight.

There is a low-temperature endotherm near 0°C

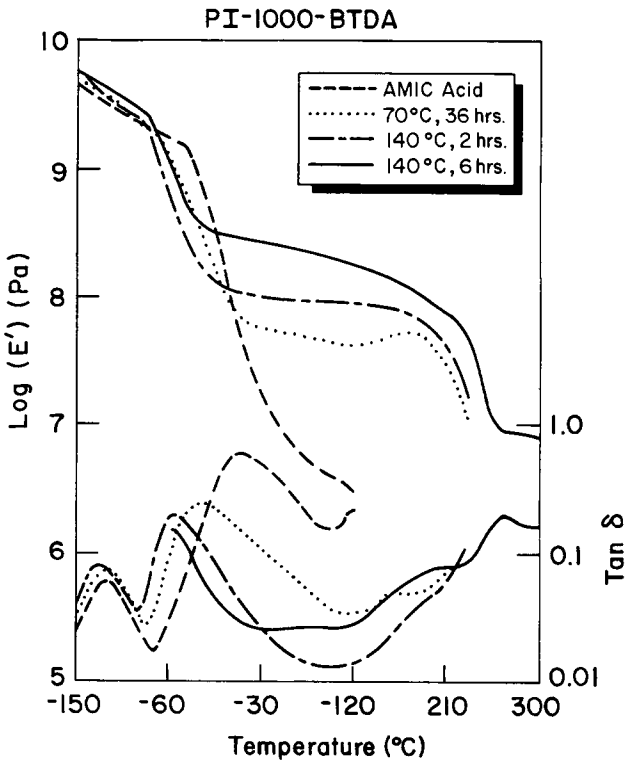

Figure 3 Dynamic mechanical analysis curves of PI-1000–BTDA after curing at different conditions. Amic acid (---); 70°C, 36 h; (· · · · · · ·); 140°C, 2 h (– · – · –); 140°C, 6 h (———).

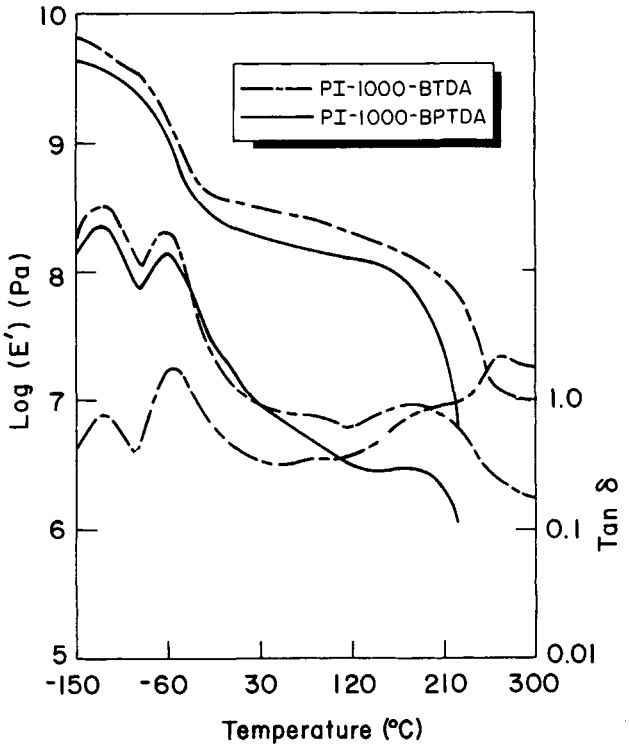

Figure 4 Dynamic mechanical analysis curves of PI-1000–BTDA (- • - • -) and PI-1000–BPTDA (———).

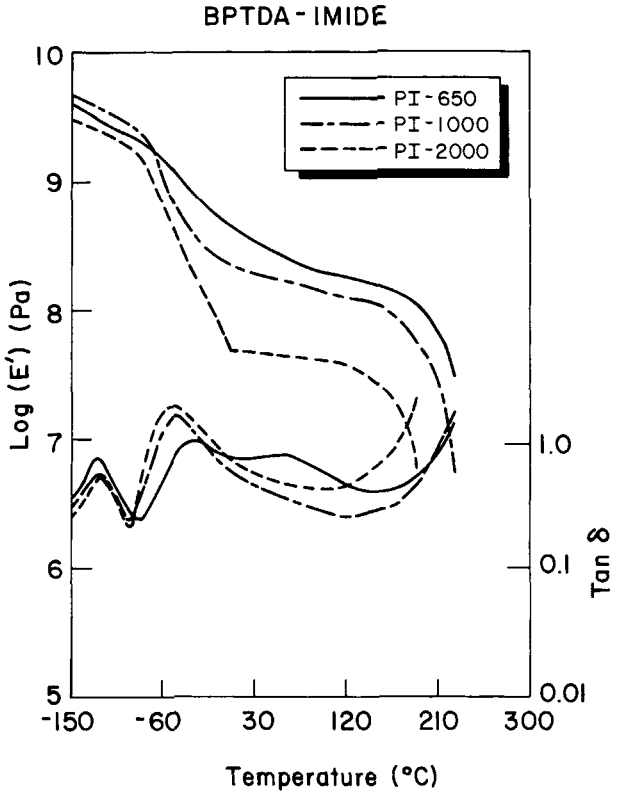

Figure 5 Dynamic mechanical analysis curves of BPTDA–imides of different soft-segment molecular weight: PI-650 (———); PI-1000 (- • - • -); PI-2000 (----).

in PI–BTDA-2000 that is attributed to the melting of PTMO crystallites. All the samples have significant hard-segment crystallinity as shown by high-temperature melting endotherms at around 200°C. The BTDA-based materials exhibit higher melting points in comparison with the BPTDA-based copolymers.

Tensile Properties

The tensile behavior of segmented polymers is generally considered to depend on the size, shape, and concentration of the hard-segment domains. Cohesive forces and intermolecular hydrogen bonds within the hard-segment microdomains also affect the tensile strength.

The stress–strain curves of both BTDA- and BPTDA-based materials are shown in Figure 7. Table III summarizes the results of the tensile measurements.

Three conclusions can be drawn from the results: First, an increase in the hard-segment content in both the BTDA- and BPTDA-based polymers leads to higher modulus and lower elongation at break. Second, in comparison with the BPTDA-based materials, the BTDA-based materials exhibit higher elongation at break, better ultimate stress, and lower Young's modulus. The former two observations can

Table II DSC Data for the Poly(ether)–Polyimides

Sample Code	T_g (°C)	Onset (°C)	End (°C)	Breadth (°C)	T_m (°C)
PI-650–BTDA	−71	−90	−44	46	262
PI-1000–BTDA	−74	−92	−56	26	247
PI-2000–BTDA	−77	−84	−68	16	189
PI-650–BPTDA	−57	−76	−38	38	202
PI-1000–BPTDA	−68	−82	−54	28	199

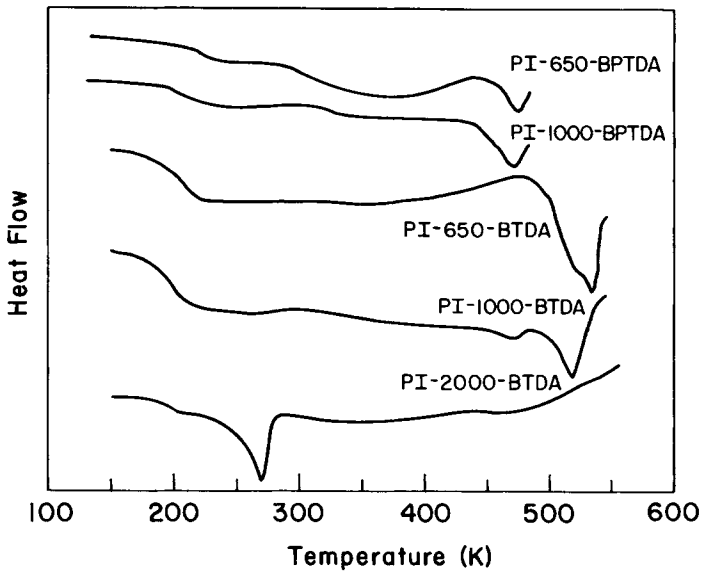

Figure 6 DSC curves of polyether–polyimides.

be attributed to the better phase separation and stronger cohesiveness of the hard-segment phase in BTDA-based materials. The lower modulus may be associated with the lower hard-segment content in the BTDA-based materials. The Young's modulus is largely determined by the rigid continuous or co-continuous phase in multiphase polymers, and the BPTDA-based polymers possess a higher hard-segment content and, hence, a higher modulus. Finally, both the BTDA- and BPTDA-based polymers with higher hard-segment contents show a yield phenomenon in their stress–strain curves. The yielding can be explained by the disruption of the hard-segment domain interconnectivity.

Figure 8 shows the mechanical property variations during the progression of the PI—BTDA-1000 imidization reaction. As the imidization conversion increases, the tensile strength increases and elongation decreases. This indicates that the imide linkages act as physical cross-links and reinforcing filler, results that are in agreement with the dynamic mechanical analysis. Figure 8 also contains the stress–strain curve of the PI–BTDA-1000 polyamic acid sodium salt. It is interesting to note that the sodium

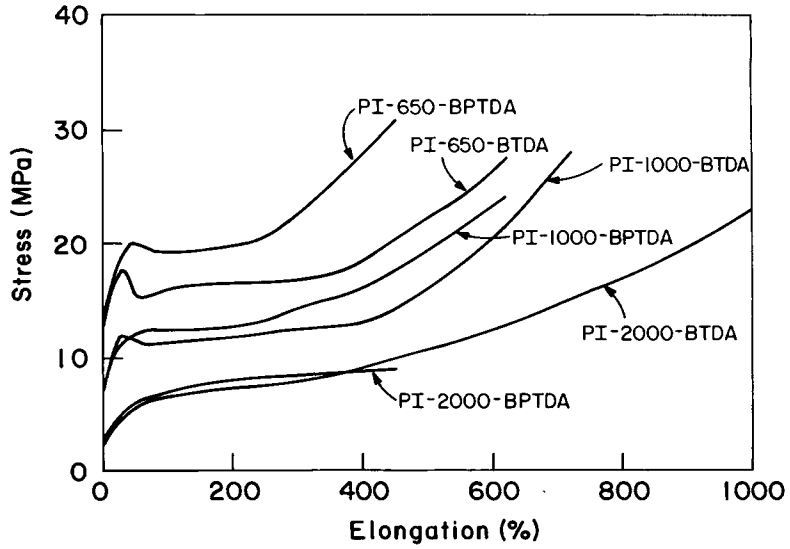

Figure 7 Uniaxial stress–strain results for the polyether–polyimides.

Table III Summary of Tensile Properties

Code	Ultimate Stress (MPa)	Elongation at Break (%)	Young's Modulus (MPa 100%)
PI-650-BTDA	31.9	659	16.0
PI-650-BPTDA	32.3	458	19.4
PI-1000-BTDA	30.4	738	11.5
PI-1000-BPTDA	25.2	640	12.5
PA-1000-BTDA-Na	30.5	387	5.8
PI-2000-BTDA	24.0	1120	6.2
PI-2000-BPTDA	9.0	470	6.8

salt of PA-BTDA-1000 also behaves as a thermoplastic elastomer. The polyether amide ionomers will be discussed in detail elsewhere.

Kinetic Study of the Imidization Reaction

Infrared spectroscopy has been widely used in kinetic studies of the thermal imidization reaction of polyamic acids. The IR absorbance bands at 1780, 1540, 1380, and 720 cm^{-1} are frequently used to monitor the appearance of imide and the disappearance of amic acid.[9-12] In the system of the polyether–amic acid block copolymer, the band at 720 cm^{-1} is most suitable for evaluating the level of imidization. The band at 1780 cm^{-1} is too weak, and the bands at 1540 and 1380 cm^{-1} are overlapped with other bands attributed to aliphatic hydrocarbon species. Absorbance intensities of the 720 cm^{-1} band were measured and ratioed to an ether C—O—C stretching vibration at the 1100 cm^{-1} reference band to normalize for variations in film thickness. A fully imidized sample was prepared at a cure temperature of 220°C (near the hard-segment T_g). The absorbance intensity of this sample did not increase as it was further heated at 260°C. Therefore, the imidization was considered to be completed. The conversion of each sample was calculated according to Beer's law. In Figure 9, the imide content is plotted against time for three reaction temperatures. It can be seen from the curves that the poly(ether amic acid) was converted into polyimide at low cure temperatures. In Figure 10, first-order kinetic plots of the imidization reaction obtained by FTIR are shown. The kinetic curves are not completely linear but are similar to the bulk imidization kinetics of typical aromatic polyamic acids.[11] Below about 60% conversion, a linear relationship is observed. The Arrhenius plot in Figure 11 was generated from the

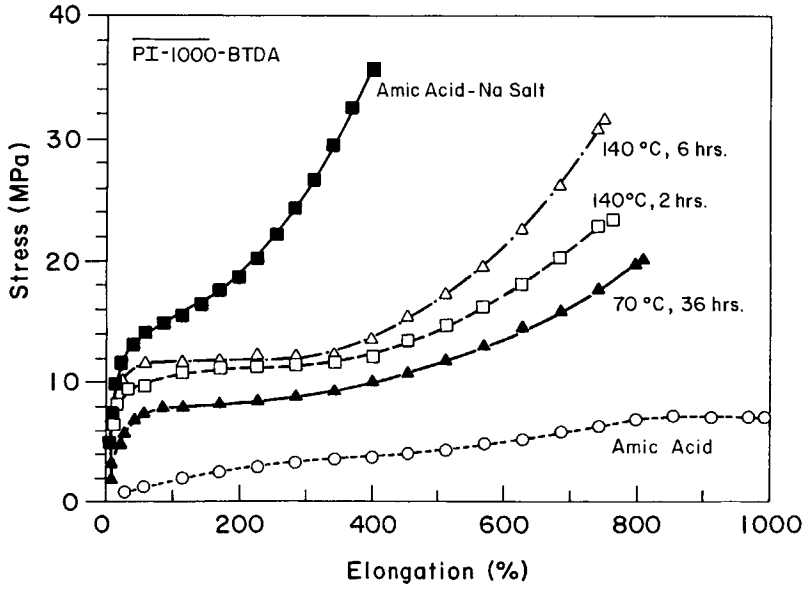

Figure 8 Uniaxial stress–strain results for PI-1000–BTDA after curing at different conditions and for the amic acid–Na salt.

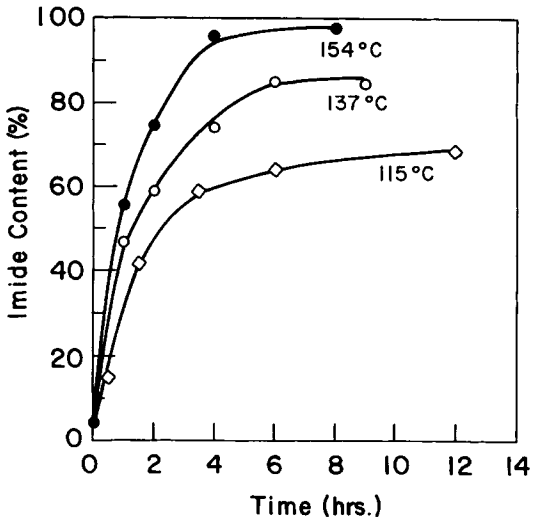

Figure 9 Plot of imide content vs. time for three different temperatures: (◇) 115°C; (○) 137°C; (o) 154°C.

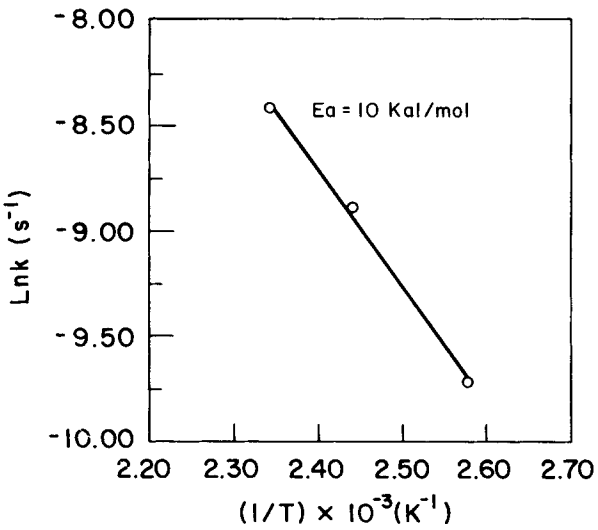

Figure 11 Arrhenius plot of the first-order reaction rate constant for the imidification reaction.

first-order rate constants. The activation energy for the imidization reaction of the block copolymers was found to be about 10 kcal/mol, much lower than that of aromatic polyamic acids.[9]

CONCLUSIONS

Polyether–polyimide block copolymers are soluble thermoplastic elastomers that exhibit a well-phase-separated morphology and possess a wide range of service temperatures. Introduction of polyether soft segments into the backbone of polyimide facilitates the imidization process. Polyether–amic acid salts are a new family of ionomers that also exhibit thermoplastic elastomer properties.

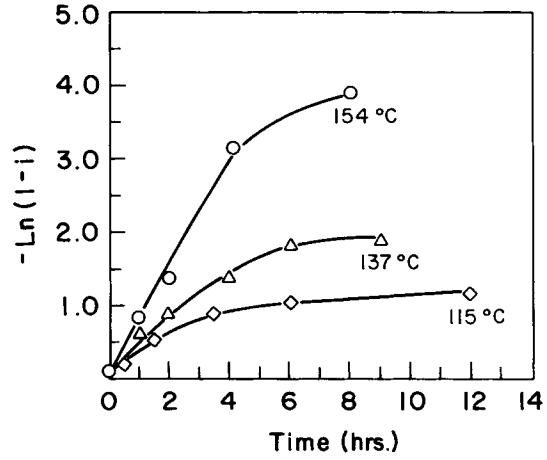

Figure 10 First-order kinetic plots of the imidization reaction: (◇) 115°C; (△) 137°C; (○) 154°C (where i = extent of reaction).

REFERENCES

1. P. E. Gibson, M. A. Vallance, and S. L. Cooper, in *Developments in Block Copolymers,* I. Goodman, Ed., Applied Science, London, 1982, pp. 217–259.
2. A. Noshay and J. E. McGrath, *Block Copolymers: Overview and Critical Survey,* Academic Press, New York, 1977.
3. M. I. Bessonov, M. M. Koton, V. V. Kudryavtsev, and L. A. Laius, *Polyimides-Thermally Stable Polymers,* Plenum Press, New York, 1987.
4. S. Tjugit and W. A. Feld, *Polym. Prepr.,* **28**(2), 205 (1987).
5. M. Navarre, in *Polyimides: Synthesis, Characterization, and Applications,* K. L. Mittal, Ed., Plenum Press, New York, 1984, Vol. 1, p. 429.
6. B. Masiulanis, J. Hrouz, J. Baldrain, M. Ilavsky, and K. Dusek, *J. Appl. Polym. Sci.,* **34,** 1941–1951 (1987).
7. I. Yilgor and J. E. McGrath, *Advances in Polymer Science,* **86,** 31(1988).
8. Y. Yoo, S. Kilic, and J. E. McGrath, *Polym. Prepr.,* **28**(2), 272 (1987).
9. R. W. Snyder, and P. C. Painter, *Polym. Mater. Sci. Eng.,* **59,** 57 (1988).
10. S. Numata, K. Fujisaki, and N. Ninjo, in *Polyimides: Synthesis, Characterization and Applications,* K. L. Mittal, Ed., Plenum Press, New York, 1984, Vol. 1, pp. 259–271.
11. J. A. Kreuz, A. L. Endrg, F. P. Gay, and C. E. Sroog, *J. Polym. Sci. A-1,* **4,** 2067 (1966).
12. J. D. Summers and J. E. McGrath, *Polym. Prepr.,* **28**(2), 230 (1987).

Received January 29, 1991
Accepted March 15, 1991